LIFETIME OF THE LUNAR DYNAMO CONSTRAINED BY YOUNG APOLLO RETURNED BRECCIAS 15015 AND 15465. H. Wang[1*], S. Mighani[1*], B. P. Weiss[1], D. L. Shuster[2,3], K. V. Hodges[4], [1]Department of Earth, Atmospheric, and Planetary Sciences, Massachusetts Institute of Technology, Cambridge, MA, USA (huapei@mit.edu), [2]Department of Earth and Planetary Science, University of California, Berkeley, CA, USA, [3]Berkeley Geochronology Center, Berkeley, CA, USA, [4]School of Earth and Space Exploration, Arizona State University, Tempe, Arizona, USA. *These authors contributed equally to this study.

Introduction: Paleomagnetic studies have shown that a dynamo magnetic field of tens of μT likely existed on the surface of the Moon from at least 4.5 to 3.6 Ga and declined to several μT by 3.3 Ga [1]. Furthermore, a recent analysis of lunar regolith breccia 15498 found that the lunar surface field persisted until at least ~1-2.5 Ga, when it had an intensity of ~5 μT at [2]. However, a key unknown is when the dynamo finally ceased. Establishing when the dynamo ended is important because it could enable discrimination between various hypothesized dynamo mechanisms. In particular, only precession and core crystallization are thought to be able to power the dynamo beyond ~3-0.6 Ga [3, 4], while only core crystallization is thought capable of supporting a dynamo beyond ~0.6 Ga [5]. Given that the Moon's core likely crystallized inward for much of its crystallization history [6], evidence in favor of core crystallization may in turn suggest that dynamos in small bodies could be powered by inward core crystallization. To constrain the late history of the lunasr dynamo, we studied the paleomagnetism of 2 young Apollo 15 returned samples 15015 and 15465.

Samples and Experiments: Regolith breccia 15015 contain ~90% melt glass matrix, which should have recorded any ambient paleomagnetic field as a thermoremanence (TRM) on the lunar surface at the time of its formation. Apollo-era $^{40}Ar/^{39}Ar$ measurements suggest that the glass formed at 1.0 ± 0.2 Ga [7], consistent with its trapped $^{40}Ar/^{36}Ar$ model age of 0.5 ± 0.4 Ga [8].

The 15465 breccia consists of angular breccia clasts welded together by a dark melt glass. The true age of this melt is still unclear, but almost certainly less than ~2 Ga. Apollo-era $^{40}Ar/^{39}Ar$ measurements by [9] were interpreted to indicate a glass formation age of 1.19 ± 0.14 Ga, while subsequent $^{40}Ar/^{39}Ar$ laser probe measurements [10] implied an imprecise glass formation age of just 130 ± 90 Ma. Fagan et al. 2014 report a trapped $^{40}Ar/^{36}Ar$ age of 1.9 ± 0.4 Ga [8].

Transmission X-ray microscopy and X-ray absorption near edge structure measurements of 15015 show that the majority of the ferromagnetic recorders within this regolith breccia are fined-grained (<~2 μm) iron particles. Hysteresis loops and a first-order reversal curves (FORC) diagram [11] of 15015 indicate a predominately pseudo-single domain (PSD) grain size signal (Fig. 1), making the young regolith breccia 15015 an exceptionally good paleomagnetic recorder among lunar rocks.

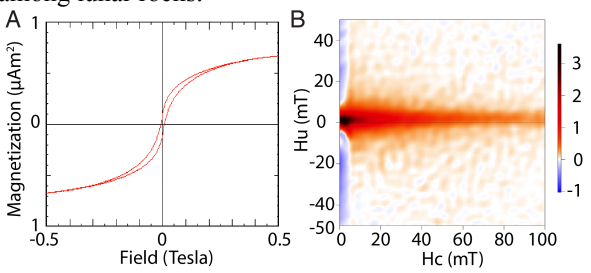

Fig. 1. (A) Paramagnetism-corrected hysteresis loop up to 1 Tesla maximum applied field, yielding saturation magnetization over induced magnetization ratio of 0.14 . (B) FORC diagram, shown is Hu (which quantifies the local interaction field) on the ordinate versus Hc (coercivity) on the abscissa. The color bar shows the probability density of hysterons belonging to a given Hu and Hc. Long and narrow central ridge (red) indicates typical fine-grained PSD signal.

Our alternating field (AF) demagnetization (Fig. 2A) and anhysteretic remanence (ARM) paleointensity experiments found that 15015 matrix glass subsamples with faces exposed to band-saw cutting at Johnson Space Center (JSC) contain highly stable and intense natural remanence (NRM) (Fig. 3A, red curve), but have NRM directions that are highly non-unidirectional across the parent sample (Fig. 3B).

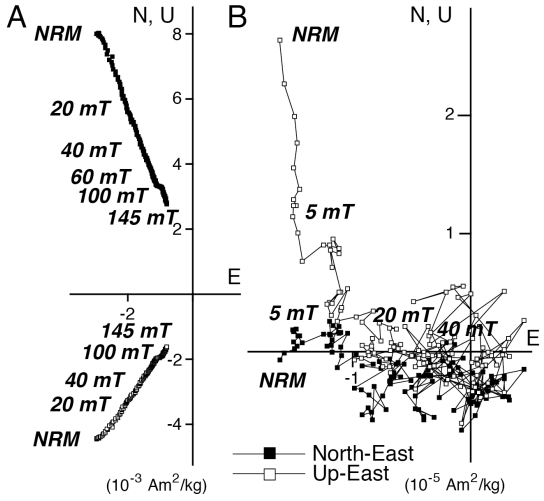

Fig. 2. AF demagnetization vector plots of (A) a 15015 sawcut face subsample 229a1v; and (B) a 15015 interior subsample 229a1m. Shown is the projection of the endpoint of the NRM onto the North-East (solid squares) and Up-East plane (empty squartes). AF demagnetization levels are labeled on plots.

Matrix glass subsamples taken away from the sawcut faces (> 5 mm depth) of 15015, as well as clast and matrix subsamples from 15465 (which was not sawn at

JSC) contain no stable NRM (Fig. 2B; Fig. 3A, blue curve) and formed in an extremely weak paleofield.

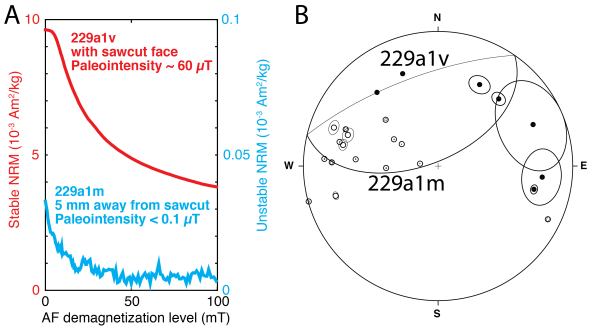

Fig. 3. (A) AF demagnetization spectra of 15015 matrix glass subsamples 229a1v (red; from JSC sawcut face) and 229a1m (blue; from interior). Notice the two order of magnitude difference in the magnitude of their NRMs and the much higher AF level required to demagnetize the sawcut sample. (B) Equal area plot of the the NRM directions of subsamples of 15015. Solid dots point down; empty dots point up. Radii of ellipses around dots are proportional to their NRM/ARM paleointensities (1º corresponds to 1 μT).

Thermal demagnetization of subsamples of 15015 with JSC sawcut faces removed their NRM by just 150ºC, indicating that their NRMs are in fact partial thermoremanence (TRM) overprints from the band-saw cutting process rather than true lunar total TRM. Thus, the lunar surface field recorded by 15015 was apparently extremely weak at ~1.0 Ga.

Paleointensity experiments using anhysteretic remanence (ARM) [12] on both 15015 and 15465 matrix glass and Thellier-Thellier double heating experiments [13] on 15015 matrix glass (Fig. 4) yield paleointensities of <0.03 ± 0.10 μT and 0.4 ± 0.5 μT (uncertainties are 95% confidence intervals). Both results indicate essentially zero-field conditions during glass formation.

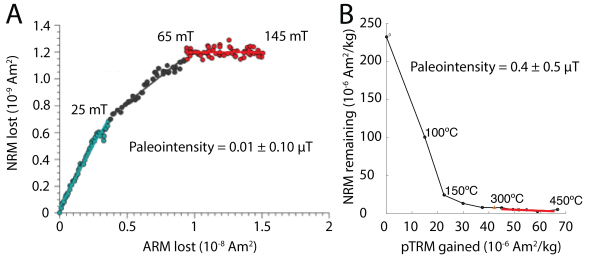

Fig. 4. (A) ARM paleointensity experiment on 15465 clast subsample 6-2. Shown is NRM lost versus ARM gained. The paleointensity calculated from AF of 65 mT to 145 mT. (B) Thellier-Thellier paleointensity experiment. Shown is the NRM remaining versus partial TRM gained for 15015 matrix glass subsample 229b8. Paleointensity is calculated from 300ºC to 450ºC. The partial TRMs for 100ºC, 150ºC, 200ºC and 250ºC are interpolated using the pTRM of 300ºC and assuming a linear increase of partial TRMs with temperature below 300ºC.

Implications: Our new paleomagnetic data for 15015 and 15465 indicate the lunar surface magnetic field dropped to <0.1 μT (ARM paleointensity constraints) at ~1 Ga (Fig. 5).

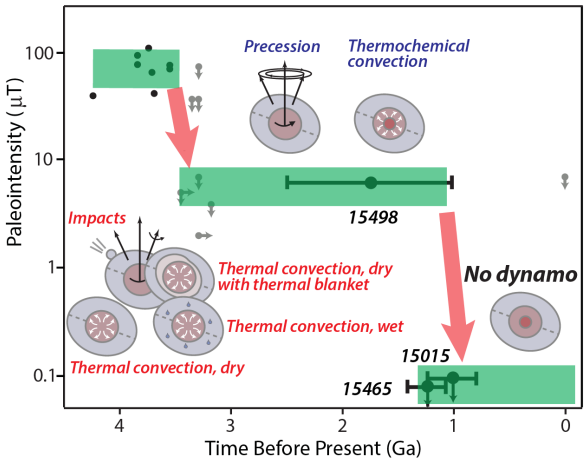

Fig. 5. Moderm lunar paleomagnetic data [1] and new results from regolith breccia 15498 [2], 15015 and 15465 (this study) show a three-stage decline of the lunar surface field (as marked by green bars) from ~10^2 μT (~4.2 Ga to ~3.6 Ga) to ~10 μT (~3.6 Ga to ~2.5-1 Ga) to <~10^{-1} μT (~2.5-1 Ga to present day). Different lunar dynamo power sources are plotted along the time axis according to their predicted lifetimes [1]. Previously reported $^{40}Ar/^{39}Ar$ ages for 15015 and 15465 are used in this plot. We are conducting bulk sample and laser probe $^{40}Ar/^{39}Ar$ dating to better constrain the magnetization ages of 15015 and 15465.

For typically assumed lunar interior parameters, essentially all published models of the lunar dynamo [5, 14, 15, 16, 17, 18] predict surface fields >0.1 μT for >~90% of the time period while the dynamo is active. Such a minimum field [19] is comparable to estimates of the strongest lunar crustal surface fields and below even the weakest known dynamo surface field in the solar system today [20]. Therefore, our 0.1 μT upper limit indicates that the lunar dynamo likely ceased sometime between ~2.5 Ga and ~1.0 Ga. This timing is consistent with both thermochemical convection due to core crystallization and mantle precession as the major power sources for the late lunar dynamo.

References: [1] Weiss, B. P. and Tikoo, S. M. (2014) Science 346, 1198. [2] Tikoo, et al. (2014) *LPSC 45*, 1972. [3] Williams, J. G. et al. (2001) *JGR 106*, 27933. [4] Smoluchowski, R. (1973) *Moon 7*, 127-131. [5] Laneuville, M. et al. (2014) *EPSL 401*, 251-260. [6] Scheinberg, A. et al. (2015) *Icarus 254*, 62-71. [7] Eglinton, et al. (1974) in *Lunar Sample Studies*, NASA SP-418. [8] Fagan, et al. (2014) *Earth Moon Planets*, 10.1007/s11038-11014-19437-11037. [9] Husain L. (1972) *Apollo 15 lunar samples 1,* 374-377. [10] Laurenzi M. A. et al (1988). *LPSC Proceedings 28,* 299-306. [11] Roberts, A. P. et al. (2000) *JGR 105*, 28461-28475. [12] Weiss, B. P. et al. (2008) *Science 322*, 713-716. [13] Thellier, E. and Thellier, O. (1959) *Ann. Geophys. 15*, 285-378. [14] Stegman, D. R. et al. (2003) *Nature 421*, 143-146. [15] Takahashi, F. and Tsunakawa, H. (2009) *GRL 36*, 1-4. [16] Le Bars, M. et al. (2011) *Nature 479*, 215-218. [17] Dwyer, C. A. et al. (2011) *Nature 479*, 212-214. [18] Tian, B. Y. et al. (2014) *AGU Fall Meeting*, Abs# GP54A-04. [19] Hemingway, D. and Garrick-Bethell I. (2012) *JGR 117*, E10012. [20] Anderson, B. J. (2010) *Space Sci. Rev. 152*, 307-339.